# The Binary Boron Trifluoride-Hydroxylamine Molecular Complex: N-Bound or O-Bound?[†]

### T. Anthony Ford*

*Centre for Theoretical and Computational Chemistry, School of Chemistry, University of KwaZulu-Natal, Westville Campus, Private Bag X54001, Durban 4000, South Africa.*

**ABSTRACT**

**Boron trifluoride acts as a classical Lewis acid in forming molecular complexes with a variety of electron donors. Recent computational results on a number of complexes with some oxygen and nitrogen bases have indicated relationships between the properties of the adducts, such as the interaction energies and the wavenumber shifts of some of the modes of the boron trifluoride sub-molecule, and some physical properties of the bases. Hydroxylamine represents an example of a base containing two potential sites of electron donation, the nitrogen and the oxygen atoms. Predictions based on our earlier investigations of systems of this type suggest that hydroxylamine would bind to boron trifluoride preferentially through its nitrogen atom. Whether such a complex adopts an equilibrium structure in which the NO bond of hydroxylamine lies *cis* or *trans* to one of the BF bonds of boron trifluoride is more difficult to predict. This paper investigates the relative binding properties of N-bound *versus* O-bound complexes of boron trifluoride with hydroxylamine, and explores the conformational preferences and vibrational spectra of both types of adduct.**

**KEYWORDS**

*Ab initio* **calculations, molecular complexes, boron trifluoride, hydroxylamine.**

## 1. Introduction

Boron trifluoride is a classical Lewis acid and forms molecular complexes with a variety of electron donors, including oxygen, nitrogen, sulphur and halogen bases.[1] Examples of our earlier *ab initio* studies of complexes formed between $BF_3$ and oxygen and nitrogen bases indicate a wide range of interaction energies, as indicated in Table 1.

Despite the variety of levels of theory and basis sets used in these calculations, and the differences in the structures of the bases, a number of generalizations are apparent. Oxygen and nitrogen atoms in the *sp* hybrid state (O-bound $CO^2$ and N-bound $N_2O^6$) tend to take part in very weak interactions. Bases containing these atoms in the $sp^2$ hybrid state (as in $H_2CO$ and $CH_2NH$) undergo medium to strong interactions. When O and N are found in the $sp^3$ hybrid state (e.g. $H_2O$,[4] $CH_3OH$, $(CH_3)_2O$,[5] $NH_3$, $CH_3NH_2$, $(CH_3)_2NH$ and $(CH_3)_3N^7$) the interactions tend to be quite strong, and the strength of interaction increases with increasing degree of methyl substitution. Moreover, for bases containing O and N atoms having the same number of methyl groups, the N bases are invariably more strongly bound than the O bases.

Nitrous oxide is the only case we have studied so far of a base which has the capability of binding through either of two different sites, the terminal nitrogen and oxygen atoms. Hydroxylamine represents a further example of a base which can interact through either its N or its O atom. In either case, two conformations are possible, with the NO bond either *cis* or *trans* to one of the BF bonds. This presentation reports the results of an *ab initio* study to ascertain the preferred structure of the boron trifluoride-hydroxylamine complex, and to compare the interaction

**Table 1** Interaction energies of the complexes formed between boron trifluoride and some oxygen and nitrogen bases.

| Oxygen bases | | Nitrogen bases | |
|---|---|---|---|
| Base | Interaction energy /kJ mol$^{-1}$ | Base | Interaction energy /kJ mol$^{-1}$ |
| CO [a] | –4.10 | N$_2$O [f] | –5.14 |
| N$_2$O [b] | –3.45 | CH$_2$NH [c] | –177.69 |
| H$_2$CO [c] | –66.16 | NH$_3$ [g] | –160.35 |
| H$_2$O [d] | –56.70 | CH$_3$NH$_2$ [g] | –191.72 |
| CH$_3$OH [e] | –97.97 | (CH$_3$)$_2$NH [g] | –209.72 |
| (CH$_3$)$_2$O [e] | –116.63 | (CH$_3$)$_3$N [g] | –217.23 |

[a] O-bound, RHF/6-31G(d), ref. 2.
[b] O-bound, MP2/6-31G(d), ref. 3.
[c] MP2/6-311++G(d,p), unpublished work, this laboratory.
[d] MP2/6-311++G(d,p), ref. 4.
[e] MP2/6-311++G(d,p), ref. 5.
[f] N-bound, MP2/6-31G(d), ref. 6.
[g] MP2/6-311++G(d,p), ref. 7.

energies and vibrational spectra of the N-bound and O-bound isomers.

To the best of our knowledge, no experimental gas phase microwave, infrared spectroscopic or *ab initio* theoretical studies of the $BF_3.NH_2OH$ complex have yet been reported, thus no previous data are available for comparison with the results reported here.

## 2. Computational Methodology

The calculations were carried out using the Gaussian 98 computer program,[8] at the second order level of Møller-Plesset perturbation theory (MP2),[9] and employing the 6-311++G(d,p) basis set.[10,11] Geometry optimizations were performed at the VERYTIGHT convergence level,[8] initially imposing $C_s$ symmetry
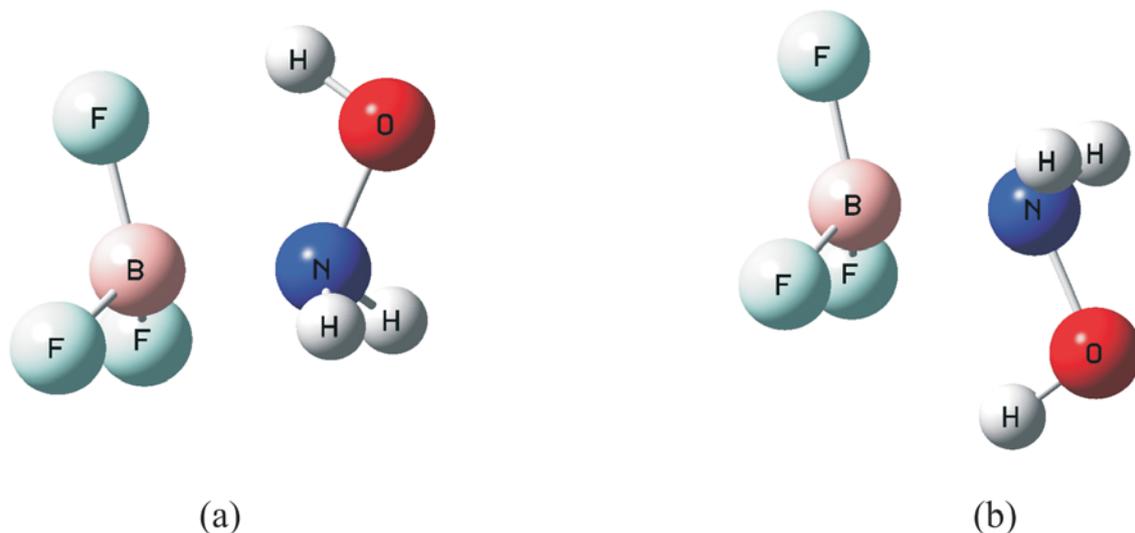
**Figure 1** The optimized $C_s$-constrained structures of the B…N bonded $BF_3.NH_2OH$ complexes; (**a**) *cis,* (**b**) *trans.*
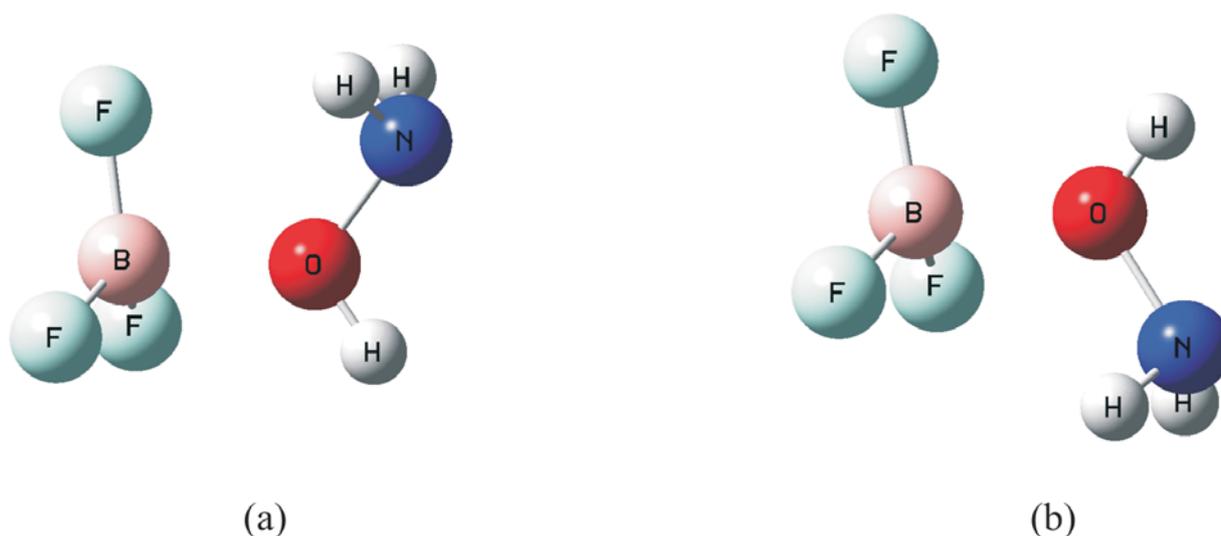


**Figure 2** The optimized $C_s$-constrained structures of the B…O bonded $BF_3.NH_2OH$ complexes; (**a**) *cis,* (**b**) *trans.*

on the structures of the complexes, and with both *cis* and *trans* starting geometries in each case. Later calculations were done on the totally relaxed N-bound and O-bound complex structures, of $C_1$ symmetry. Vibrational analyses were executed using the FREQ keyword,[8] using analytical derivatives. Interaction energies were calculated from the minimized energies of each complex and of the relaxed structures of the monomers in the complexes, and were corrected for basis set superposition error (BSSE),[12] employing the Boys-Bernardi full counterpoise correction procedure,[13] and for zero-point energy differences.

## 3. Results and Discussion

The four optimized $C_s$ structures, *cis* and *trans* N-bonded and *cis* and *trans* O-bonded, of the $BF_3.NH_2OH$ complex are shown in

Figs 1 and 2. Table 2 reports the minimized energies of these four structures, and their Hessian indices. This table indicates that both N-bound isomers are more stable than the O-bound counterparts, and that, while the *cis* N-bound structure has a lower energy than the *trans,* the order of energies is reversed for the O-bound species. Of more significance in Table 2, however, is the fact that all four isomers are transition states; in the case of the *cis* O-bound a second order transition state. These observations indicate that the true structures of both the N-bound and the O-bound complexes are of lower symmetry, and the expectation that the preferred structures contained a plane of symmetry was unjustified.

The two basic structures were therefore subjected to a potential surface scan, the energies being computed with the ONBF or

**Table 2** Minimized energies and Hessian indices of the isomers of the $BF_3.NH_2OH$ complex.

| | N-bound | | | O-bound | |
| --- | --- | --- | --- | --- | --- |
| Structure | Energy/H | Hessian index | Structure | Energy/H | Hessian index |
| *cis*, $C_s$ | –455.4511 | 1 | *cis*, $C_s$ | –455.4284 | 2 |
| *trans*, $C_s$ | –455.4501 | 1 | *trans*, $C_s$ | –455.4305 | 1 |
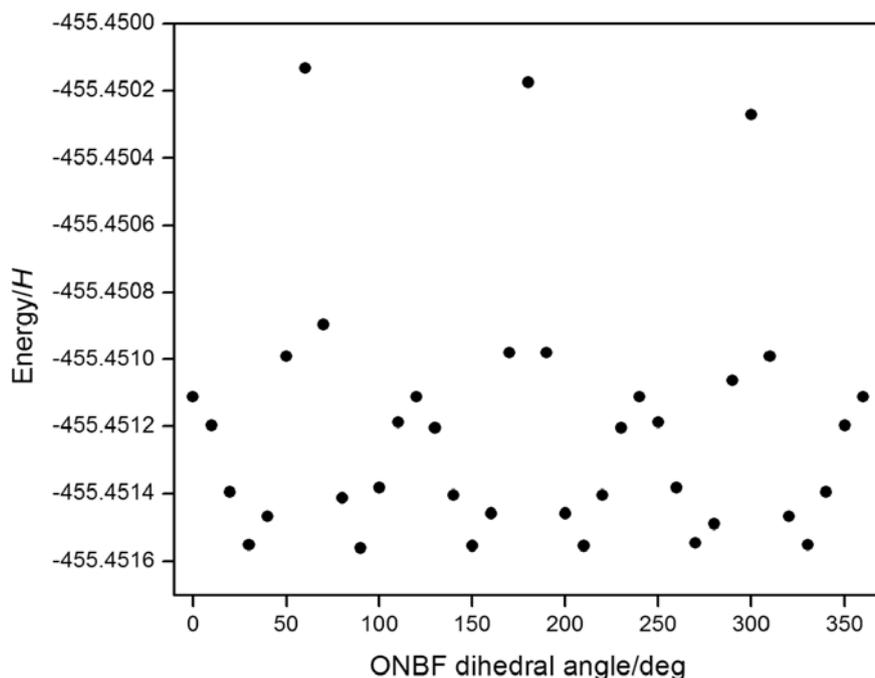
**Figure 3** Plot of the energy of the N-bound $BF_3.NH_2OH$ complex as a function of the ONBF dihedral angle.

NOBF dihedral angles fixed at values varying from 0 to 360 ° in 10 ° increments, while allowing all other geometrical parameters to vary freely. The potential surface scans are illustrated in Figs 3 and 4.

Figure 3 indicates that the plot for the N-bound species is symmetric about 180 °, with six equivalent minima at about 30, 90, 150, 210, 270 and 330 °, three main maxima at 60, 180 and 300 ° (the *trans* structures) and three subsidiary maxima at the *cis* positions (0, 120 and 240 °). In the case of O-bound $BF_3.NH_2OH$, the plot is unsymmetrical, with two main minima near 40 and 200 °, two secondary minima at about 90 and 290 °, and with four maxima at approximately 80, 150, 270 and 330 ° (Fig. 4). Unrestricted geometry optimizations, with the $C_s$ constraints

removed, yielded the converged structures shown in Fig. 5. Figure 5a shows a tilt of about 30 ° of the BNO plane of the N-bound structure (**1**) relative to the FBN plane (near the *cis* conformation), and in the case of the O-bound structure (**2**) shown in Fig. 5b, the BON plane is displaced by *ca.* –160 ° with respect to the FBO plane (close to the *trans* structure). The preference of the N-bound isomer for the (approximately) *cis* conformation is explained by a secondary electrostatic attraction of the hydroxyl hydrogen atom for one of the fluorine atoms, in a cyclic five-membered OH…F hydrogen-bonded arrangement. By contrast, the preferred conformation of the O-bound isomer is the (approximately) *trans*, since an intramolecular OH…F hydrogen-bonded interaction in this case would require a
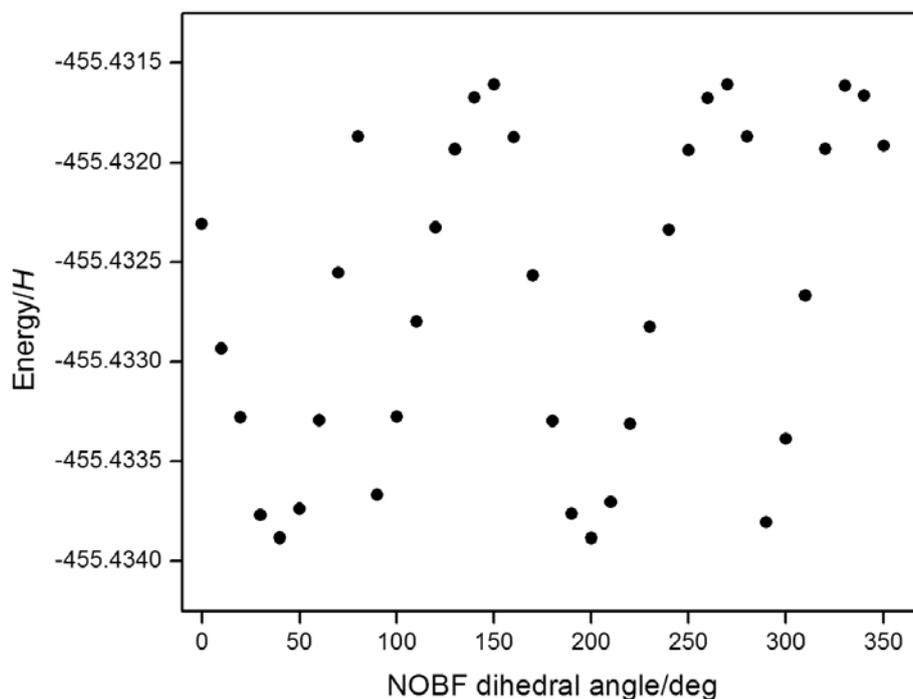


**Figure 4** Plot of the energy of the O-bound $BF_3.NH_2OH$ complex as a function of the NOBF dihedral angle.
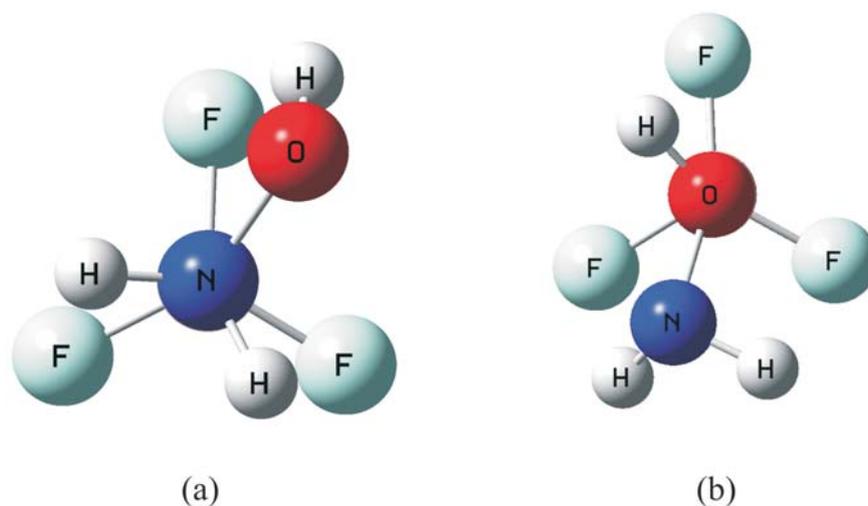
**Figure 5** The optimized structures of the (**a**) B…N bonded (**1**) and (**b**) B…O bonded (**2**) BF$_3$.NH$_2$OH complexes projected along the B…N and B…O axes.

**Table 3** Minimized energies and Hessian indices of the global minima of the BF$_3$.NH$_2$OH complex.

| | N-bound | | | O-bound | |
|---|---|---|---|---|---|
| Structure | Energy/$H$ | Hessian index | Structure | Energy/$H$ | Hessian index |
| **1** | –455.4516 | 0 | **2** | –455.4339 | 0 |

four-membered ring, which would involve unfavourably bent hydrogen bond angles. The stability of the O-bound isomer can then be rationalized by a secondary interaction between the amino hydrogen atoms and two of the fluorine atoms. The appearance of six minima for the N-bound species, but only four for the O-bound, is due to the fact that the secondary OH…F interaction in the first case may be accommodated in any of six ways (interaction with any of three equivalent fluorine atoms, with equal positive and negative dihedral angles of the HON plane relative to the three NBF planes in each case), leading to a six-fold periodicity in the rotation of the BF$_3$ molecule about the B…N axis. In the second case, the subsidiary interaction between the two amino hydrogen atoms and two of the fluorine atoms may be achieved in any of four ways, defined by the four approximately equivalent combinations of the HOBF and the two HNOB dihedral angles.

The minimized energies and Hessian indices of the converged structures are listed in Table 3, which indicates substantial energy recoveries compared with the constrained C$_s$ species (Table 2), and confirms that the fully optimized structures are indeed genuine minima on the potential energy surface. The N-bound complex **1** is about 17.7 $mH$ (46.5 kJ mol$^{-1}$) more stable than the O-bound counterpart **2**.

### 3.1. Interaction Energies

The interaction energies of the two isomers, corrected for BSSE[12] and for zero-point energy differences, are presented in Table 4. This table confirms the preference of the N-bound complex relative to the O-bound.

### 3.2. Geometrical Parameters

The perturbations of the BF bond lengths and the FBF bond angles resulting from formation of the complexes are shown in Table 5.

The bond lengths all undergo a lengthening, indicating a weakening of the intramolecular bonds accompanying the

**Table 4** Interaction energies of the preferred N-bound and O-bound complexes, corrected for basis set superposition error and zero-point energy differences.

| Complex | Interaction energy/kJ mol$^{-1}$ |
|---|---|
| N-bound (**1**) | –158.79 |
| O-bound (**2**) | –83.03 |

**Table 5** Changes in the BF bond lengths and FBF bond angles on complexation.

| N-bound complex (**1**) | | O-bound complex (**2**) | |
|---|---|---|---|
| Bond lengths /pm | Bond angles /deg | Bond lengths /pm | Bond angles /deg |
| 6.84 | –4.93 | 4.92 | –2.12 |
| 5.33 | –5.33 | 3.67 | –4.01 |
| 5.12 | –6.24 | 3.45 | –5.14 |

formation of the intermolecular bonds. The bond length increases for structure **1** are uniformly larger than for **2**, consistent with the greater interaction energy. The deviations of the bond angles from the value of 120 ° found in the unperturbed monomer as the BF$_3$ structure tends towards pyramidal are also

**Table 6** Intermolecular geometrical parameters.

| N-bound complex (**1**) | | O-bound complex (**2**) | |
|---|---|---|---|
| Parameter | Value | Parameter | Value |
| R(B…N)/pm | 167.45 | R(B…O)/pm | 172.01 |
| ∠FB…N/deg | 103.79 | ∠FB…O/deg | 101.33 |
| ∠B…NO/deg | 113.96 | ∠B…ON/deg | 117.27 |
| ∠B…NH/deg | 110.15 | ∠B…OH/deg | 112.05 |

**Table 7** Computed wavenumbers and descriptions of the normal modes of the N-bound and O-bound $BF_3.NH_2OH$ complexes. (All modes are of $a$ symmetry.)

| | N-bound (**1**) | | | O-bound (**2**) | |
|---|---|---|---|---|---|
| Mode | Wavenumber/cm$^{-1}$ | Approximate description | Mode | Wavenumber/cm$^{-1}$ | Approximate description |
| $\nu_1$ | 3754.6 | $\nu$(OH) | $\nu_1$ | 3825.8 | $\nu$(OH) |
| $\nu_2$ | 3573.9 | $\nu_a$(NH$_2$) | $\nu_2$ | 3609.9 | $\nu_a$(NH$_2$) |
| $\nu_3$ | 3482.3 | $\nu_s$(NH$_2$) | $\nu_3$ | 3497.3 | $\nu_s$(NH$_2$) |
| $\nu_4$ | 1658.6 | $\delta$(NH$_2$) | $\nu_4$ | 1677.2 | $\delta$(NH$_2$) |
| $\nu_5$ | 1526.2 | $\delta$(NOH) | $\nu_5$ | 1424.5 | $\delta$(NOH) |
| $\nu_6$ | 1357.7 | tw(NH$_2$) | $\nu_6$ | 1370.8 | tw(NH$_2$) |
| $\nu_7$ | 1303.9 | $\omega$(NH$_2$) | $\nu_7$ | 1284.6 | $\nu_a$(BF$_3$) |
| $\nu_8$ | 1234.6 | $\nu_a$(BF$_3$) | $\nu_8$ | 1244.0 | $\nu_a$(BF$_3$) |
| $\nu_9$ | 1189.6 | $\nu_a$(BF$_3$) | $\nu_9$ | 1214.7 | $\omega$(NH$_2$) |
| $\nu_{10}$ | 1066.1 | $\nu$(NO) | $\nu_{10}$ | 979.3 | $\nu$(NO) |
| $\nu_{11}$ | 886.2 | $\nu_s$(BF$_3$) | $\nu_{11}$ | 831.5 | $\nu_s$(BF$_3$) |
| $\nu_{12}$ | 809.8 | geared libration | $\nu_{12}$ | 679.5 | $\tau$(NO) |
| $\nu_{13}$ | 691.0 | $\delta_s$(BF$_3$) | $\nu_{13}$ | 622.1 | $\delta_s$(BF$_3$) |
| $\nu_{14}$ | 570.0 | geared libration | $\nu_{14}$ | 511.3 | geared libration |
| $\nu_{15}$ | 480.8 | $\tau$(NO) | $\nu_{15}$ | 465.9 | $\delta_a$(BF$_3$) |
| $\nu_{16}$ | 441.9 | $\delta_a$(BF$_3$) | $\nu_{16}$ | 408.8 | $\delta_a$(BF$_3$) |
| $\nu_{17}$ | 434.8 | $\delta_a$(BF$_3$) | $\nu_{17}$ | 327.8 | geared libration |
| $\nu_{18}$ | 335.0 | $\nu$(B…N) | $\nu_{18}$ | 285.7 | $\nu$(B…O) |
| $\nu_{19}$ | 286.8 | antigeared libration | $\nu_{19}$ | 252.2 | antigeared libration |
| $\nu_{20}$ | 219.9 | antigeared libration | $\nu_{20}$ | 191.4 | antigeared libration |
| $\nu_{21}$ | 68.8 | $\tau$(B…N) | $\nu_{21}$ | 70.0 | $\tau$(B…O) |

consistently larger for the N-bound isomer. The intermolecular geometrical parameters also confirm the stronger interaction in **1** relative to **2** (see Table 6). The shorter B…N distance, indicating tighter binding, and the larger FB…N angle, resulting from a greater deviation from planarity of the BF$_3$ fragment, are quite consistent.

### 3.3. Vibrational Spectra

The vibrational analyses of the two complex isomers yield the computed wavenumbers shown in Table 7. There are some substantial differences between the wavenumbers of corresponding modes in the two isomers. In particular, the torsion about the NO bond lies 198.7 cm$^{-1}$ higher in the O-bound species, **2**. This is associated with the hydrogen-bonded interaction of the amino hydrogen atoms with two of the fluorine atoms (see above). Also, the NOH bending mode is 101.7 cm$^{-1}$ higher in the N-bound complex, **1**, due to the interaction between the hydroxyl hydrogen atom and the closest of the three fluorine atoms (see above).

The complex-monomer wavenumber shifts of the BF$_3$ sub-molecules are presented in Table 8. The BF$_3$ wavenumber shifts are all to the red, with the sole exception of that of the symmetric stretching mode of **1**. The shifts to lower wavenumber are consistent with a weakening of the intramolecular

**Table 8** Wavenumber shifts of the BF$_3$ fragments of the N-bound (**1**) and O-bound (**2**) complexes.

| BF$_3$ monomer mode | Wavenumber shift/cm$^{-1}$ | |
|---|---|---|
| | N-bound (**1**) | O-bound (**2**) |
| $\nu_s$(BF$_3$) | 12.3 | –42.4 |
| $\delta_s$(BF$_3$) | –4.3 | –73.2 |
| $\nu_a$(BF$_3$) | –199.4, –244.4 | –149.4, –190.0 |
| $\delta_a$(BF$_3$) | -32.9, –40.0 | –8.9, –66.0 |

bonds, paralleling the lengthening of those bonds as indicated in Table 5. The mean antisymmetric stretching shift of complex **1** is larger than that for complex **2**, as expected, based on our experience of this mode being the most reliable probe of the strength of interaction among the BF$_3$ complexes we have studied.[1] The symmetric bending shift, however, is significantly higher in **2** than in **1**. This is surprising, and taken together with the observation that the symmetric stretching shift of complex **1** is actually to the blue, it warrants further examination. The explanation for this anomaly is to be found in the natures of these modes in the complexes. Table 9 reports the approximate potential energy distributions of those modes nominally described in Table 7 as intramolecular BF$_3$ modes, derived from the sums of the squares

**Table 9** Approximate potential energy distributions of the intramolecular modes of the BF$_3$ fragments of the preferred N-bound and O-bound complexes.

| | N-bound (**1**) | | | O-bound (**2**) | |
|---|---|---|---|---|---|
| Complex mode | Monomer mode | Percentage PED | Complex mode | Monomer mode | Percentage PED |
| $\nu_8$ | $\nu_a$(BF$_3$) | 43 | $\nu_7$ | $\nu_a$(BF$_3$) | 21 |
| $\nu_9$ | $\nu_a$(BF$_3$) | 63 | $\nu_8$ | $\nu_a$(BF$_3$) | 87 |
| $\nu_{11}$ | $\nu_s$(BF$_3$) | 85 | $\nu_{11}$ | $\nu_s$(BF$_3$) | 76 |
| $\nu_{13}$ | $\delta_s$(BF$_3$) | 54 | $\nu_{13}$ | $\delta_s$(BF$_3$) | 95 |
| $\nu_{16}$ | $\delta_a$(BF$_3$) | 36 | $\nu_{15}$ | $\delta_a$(BF$_3$) | 33 |
| $\nu_{17}$ | $\delta_a$(BF$_3$) | 14 | $\nu_{16}$ | $\delta_a$(BF$_3$) | 21 |

of the atomic displacement coordinates for each mode for the $BF_3$ and the $NH_2OH$ fragments. Table 9 shows that the symmetric stretching vibration of adduct **1** is 85 % localized in the $BF_3$ fragment, while the symmetric bending has only a 54 % contribution from the $BF_3$ sub-molecule. Both of these modes, in both the N-bound and the O-bound cases, are strongly coupled with the B…N or B…O stretching vibration, so the assignments of the modes in Table 7 as predominantly intramolecular modes is an oversimplification, and their shifts are not directly comparable. The contributions of the $BF_3$ fragments to the antisymmetric bending modes are even lower, and less characteristic.

A comparison of the intermolecular wavenumbers of the two complexes is given in Table 10. The B…N stretching is higher that the B…O, although the B…N and B…O torsional wavenumbers are virtually identical. Correcting for the differences in the structures of the hydroxylamine sub-molecule in the complexes, by calculating the stretching and torsional force constants (see Table 11), emphasizes the relatively stronger binding in complex **1** than in complex **2**; both force constants are significantly higher for the N-bound than the O-bound complex. The librational modes, too, particularly the geared librations, have systematically higher wavenumbers in species **1**.

### 3.4. Molecular Orbital Properties

The surprising observation that the preferred structures of both isomers lack a plane of symmetry may be rationalized on the basis of the symmetry properties of the molecular orbitals of the interacting monomers. Table 12 presents the energies and symmetries of the monomer orbitals, with approximate descriptions of the natures of the orbitals, and the HOMO-1, HOMO, LUMO and LUMO+1 are pictured in Figs. 6 and 7. The primary interaction is a donation of charge from the N or O lone pair orbitals of $NH_2OH$ to the $\pi^*$ orbital of $BF_3$. In the case of com-

**Table 10** Wavenumbers of the intermolecular modes of the $BF_3.NH_2OH$ complexes.

| N-bound (**1**) | | O-bound (**2**) | |
|---|---|---|---|
| B…N stretching | 335.0 | B…O stretching | 285.7 |
| B…N torsion | 68.8 | B…O torsion | 70.0 |
| geared libration | 809.8 | geared libration | 511.3 |
| geared libration | 570.0 | geared libration | 327.8 |
| antigeared libration | 286.8 | antigeared libration | 252.2 |
| antigeared libration | 219.9 | antigeared libration | 191.4 |

**Table 11** B…N and B…O stretching and ON…BF and NO…BF torsional force constants of the N-bound and O-bound complexes.

| Force constant | Force constant/N m$^{-1}$ | |
|---|---|---|
| | N-bound complex (**1**) | O-bound complex (**2**) |
| stretching | 208.6 | 125.9 |
| torsional | 21.0 | 8.0 |

plex **1**, this involves an interaction between HOMO (n(N), 7a′) of $NH_2OH$ and LUMO+1 ($\pi^*$(BF), 2a$_2$″) of $BF_3$, and for complex **2**, between HOMO-1 (n(O), 2a″) of $NH_2OH$ and LUMO+1 (2a$_2$″) of $BF_3$. These structures are stabilized by a secondary charge donation from HOMO (n(F), 1a$_2$′) of $BF_3$ to LUMO+1 ($\sigma^*$(OH), 9a′) of $NH_2OH$ (complex **1**), and from HOMO-1 (n(F), 1e″) of $BF_3$ to LUMO ($\sigma^*$(NH), 8a′) of $NH_2OH$ (complex **2**). Alignment of the appropriate phases of the lobes of these interacting orbitals for maximum overlap requires the symmetry plane of the $NH_2OH$ sub-molecule, in either complex, to be tilted relative to one of the symmetry planes of the $BF_3$ fragment, thus lowering the overall symmetry of the complex to $C_1$.



(a)

(b)

(c)

(d)
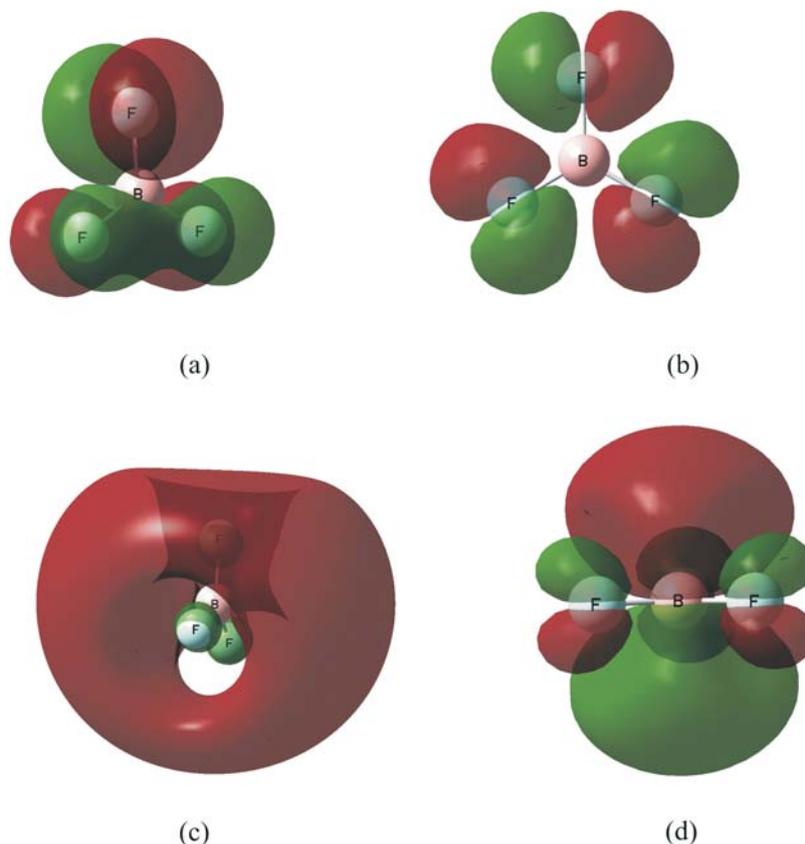
**Figure 6** Frontier orbitals of $BF_3$: (**a**) HOMO-1; (**b**) HOMO; (**c**) LUMO; (**d**) LUMO+1. Orientations are arranged for optimal viewing.

**Table 12** Properties of the molecular orbitals of the BF$_3$ and NH$_2$OH monomers.

| | BF$_3$ | | | | NH$_2$OH | | |
|---|---|---|---|---|---|---|---|
| No. | Symmetry | Energy/$H$ | Approximate description | No. | Symmetry | Energy/$H$ | Approximate description |
| 1,2 | 1e′ | -26.35348 | core(F) | 1 | 1a′ | -20.58916 | core(O) |
| 3 | 1a$_1$′ | -26.35345 | core(F) | 2 | 2a′ | -15.60887 | core(N) |
| 4 | 2a$_1$′ | -7.80405 | core(B) | 3 | 3a′ | -1.40088 | $\sigma$(NO) |
| 5 | 3a$_1$′ | -1.69345 | n(F)(2s) | 4 | 4a′ | -1.08461 | $\sigma$(NH) |
| 6,7 | 2e′ | -1.65136 | n(F)(2s) | 5 | 1a″ | -0.69306 | $\sigma$(NH) |
| 8 | 4a$_1$′ | -0.86429 | $\sigma$(BF) | 6 | 5a′ | -0.67923 | $\sigma$(OH) |
| 9,10 | 3e′ | -0.81818 | $\sigma$(BF) | 7 | 6a′ | -0.62130 | n(O)(2p$_y$) |
| 11 | 1a$_2$″ | -0.76686 | $\pi$(BF) | 8 | 2a″ | -0.48557 | n(O)(2p$_z$) |
| 12,13 | 4e′ | -0.70515 | n(F)(2p$_x$,2p$_y$) | 9 | 7a′ | -0.43152 | n(N)(2p$_x$) |
| 14,15 | 1e″ | -0.69156 | n(F)(2p$_z$) | 10 | 8a′ | 0.04635 | $\sigma$*(NH) |
| 16 | 1a$_2$′ | -0.66673 | n(F)(2p$_x$,2p$_y$) | 11 | 9a′ | 0.06383 | $\sigma$*(OH) |
| 17 | 5a$_1$′ | 0.05117 | $\sigma$*(BF) | 12 | 3a″ | 0.07383 | $\sigma$*(NH) |
| 18 | 2a$_2$″ | 0.06829 | $\pi$*(BF) | 13 | 10a′ | 0.15310 | $\sigma$*(NO) |
| 19,20 | 5e′ | 0.07996 | $\sigma$*(BF) | | | | |



(a)  (b)

(c)  (d)
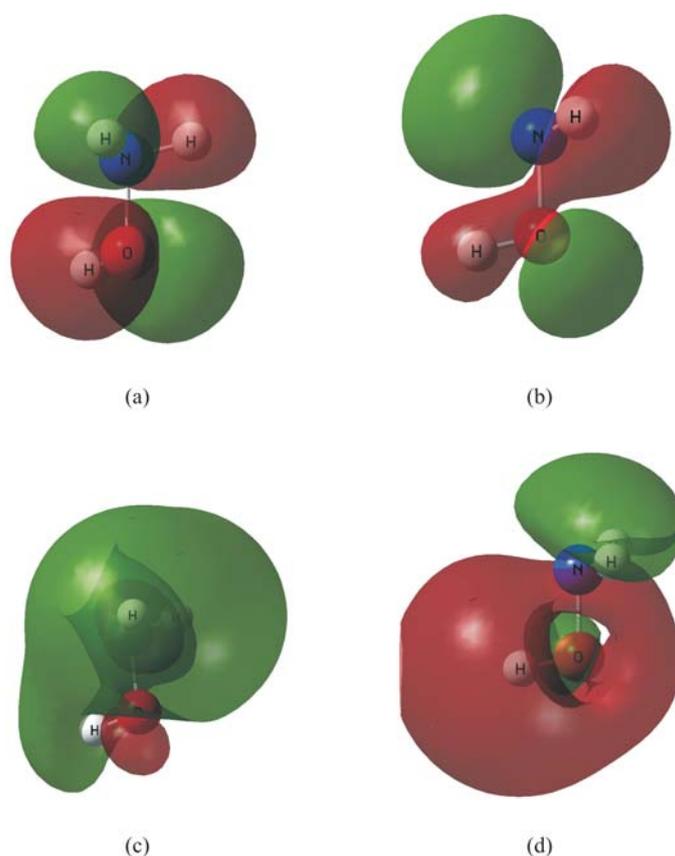
**Figure 7** Frontier orbitals of NH$_2$OH: (**a**) HOMO-1; (**b**) HOMO; (**c**) LUMO; (**d**) LUMO+1. Orientations are arranged for optimal viewing.

## References

1  T.A. Ford, Molecular complexes: perturbations of vibrational spectra, in *Encyclopaedia of Computational Chemistry* (online edition), (P. von R. Schleyer, H.F. Schaefer III, P.R. Scheiner, W.L. Jorgensen, W. Thiel and R.C. Glen, eds.), John Wiley and Sons, Chichester, UK. Article online posting date 15 June 2004. DOI: 10.1002/0470845015.cu0033.

2  L.M. Nxumalo and T.A. Ford, *S. Afr. J. Chem.*, 1995, **48**, 30–38.

3  L.M. Nxumalo, G.A. Yeo and T.A. Ford, *S. Afr. J. Chem.*, 1998, **51**, 25–34.

4  G.A. Yeo and T.A. Ford, *S. Afr. J. Chem.*, 2006, **59**, 129–134.

5  T.A. Ford, *J. Mol. Structure,* 2007, **834–836**, 30–41.

6  L.M. Nxumalo, M. Andrzejak and T.A. Ford, *J. Chem. Inf. Comput. Sci.*, 1996, **36**, 377–384.

7   F. Gaffoor and T.A. Ford, *Spectrochim. Acta, Part A*, in press. Article online posting date 17 January 2008. DOI: 10.1016/j.saa.2008.01.014.

8   Gaussian-98, Rev. A.7, M.J. Frisch, G.W. Trucks, H.B. Schlegel, G.E. Scuseria, M.A. Robb, J.R. Cheeseman, V.G. Zakrzewski, J.A. Montgomery, jr., R.E. Stratmann, J.C. Burant, S. Dapprich, J.M. Millam, A.D. Daniels, K.N. Kudin, M.C. Strain, O. Farkas, J. Tomasi, V. Barone, M. Cossi, R. Cammi, B. Mennucci, C. Pomelli, C. Adamo, S. Clifford, J. Ochterski, G.A. Petersson, P.Y. Ayala, Q. Cui, K. Morokuma, D.K. Malick, A.D. Rabuck, K. Raghavachari, J.B. Foresman, J. Cioslowski, J.V. Ortiz , A.G. Baboul, B.B. Stefanov, G. Liu, A. Liashenko, P. Piskorz, I. Komaromi, R. Gomperts, R.L. Martin, D.J. Fox, T. Keith, M.A. Al-Laham, C.Y. Peng, A. Nanayakkara, C. Gonzalez, M. Challacombe, P.M.W. Gill, B. Johnson, W. Chen, M.W. Wong, J.L. Andres, M. Head-Gordon, E.S. Replogle and J.A. Pople, Gaussian, Inc., Pittsburgh, PA, USA, 1998.

9   C. Møller and M.S. Plesset, *Phys. Rev.,* 1934, **46**, 618–622.

10  R. Krishnan, J.S. Binkley, R. Seeger and J.A. Pople, *J. Chem. Phys.,* 1980, **72**, 650–654.

11  T. Clark, J. Chandrasekhar, G.W. Spitznagel and P. von R. Schleyer, *J. Comput. Chem.,* 1983, **4**, 294–301.

12  B. Liu and A.D. McLean, *J. Chem. Phys.,* 1973, **59**, 4557–4558.

13  S.F. Boys and F. Bernardi, *Mol. Phys.,* 1970, **19**, 553–556.